



Contents lists available at ScienceDirect

# Journal of Quantitative Spectroscopy & Radiative Transfer

journal homepage: [www.elsevier.com/locate/jqsrt](http://www.elsevier.com/locate/jqsrt)

## Effective refractive index for determining ray propagation in an absorbing dielectric particle

Ping Yang <sup>a,\*</sup>, K.N. Liou <sup>b</sup><sup>a</sup> Department of Atmospheric Sciences, Texas A&M University, College Station, TX 77845, USA<sup>b</sup> Department of Atmospheric and Oceanic Sciences, Joint Institute for Regional Earth System Science and Engineering, University of California, Los Angeles, CA 90095, USA

### ARTICLE INFO

#### Article history:

Received 21 September 2008

Received in revised form

4 November 2008

Accepted 5 November 2008

#### Keywords:

Ray-tracing

Absorbing particle

Higher-order reflection–refraction events

Effective refractive indices

### ABSTRACT

The ray-tracing technique can be employed to simulate the scattering of light by a dielectric particle whose characteristic dimension is much larger than the incident wavelength. When a scattering particle is absorptive, a localized electromagnetic wave refracted into the scatterer is inhomogeneous, which requires the use of an effective refractive index to determine the propagation direction of the refracted ray. The effective refractive index for the first-order reflection–refraction event (i.e., the case for the ray-transmission from air into a particle) has been previously derived by the authors. In this study, we further develop recurrence formulae for the effective refractive indices associated with higher-order reflection–refraction events when the ray-transmission is from a particle to air. It is shown from the new formulae that effective refractive indices in this case depend upon ray history. Numerical results indicate that the real and imaginary parts of the effective refractive index are larger and smaller, respectively, than the real and imaginary parts of the inherent complex refractive index of an absorbing particle. Furthermore, if the particle faces associated with two sequential internal reflections are parallel to each other, the corresponding effective refractive indices are the same.

© 2008 Elsevier Ltd. All rights reserved.

### 1. Introduction

A number of methods have been developed to solve for the single-scattering properties of micron-sized nonspherical particles that are present in nature (e.g., ice crystals within cirrus clouds) [1]. When a particle is much larger than the incident wavelength, the ray-tracing technique based on the principles of geometric optics can be applied to solve for its optical properties. In particular, the conventional ray-tracing technique and its modification and improvement have been extensively used to investigate the single-scattering properties, including the scattering phase matrix, extinction cross section, and single-scattering albedo of nonspherical and irregular ice crystals [2–10] as well as coarse-mode dust particles [11,12].

When a scattering particle is absorptive for which the index of refraction is a complex quantity, electromagnetic waves refracted into a particle are inhomogeneous such that the planes of constant phase deviate from those of constant amplitude [13]. In this case, Snell's law, if expressed in terms of a complex refractive index, would involve a complex angle that does not have a simple geometric meaning and cannot be applied to ray-tracing analysis. To circumvent this difficulty,

\* Corresponding author. Tel.: +1979 845 4923.

E-mail address: [pyang@ariel.met.tamu.edu](mailto:pyang@ariel.met.tamu.edu) (P. Yang).

Yang and Liou [14] introduced an effective refractive index and formulated Snell's law in such a manner that complex quantities are not required. However, the previous study was limited to the first-order reflection–refraction event when the transmission of a ray is from air into a particle. For higher-order reflection–refraction events when the transmission of a ray is from a particle to air, the effective refractive index associated with the first-order reflection–refraction event was used as an approximation. In this study, we revisit this issue and derive effective refractive indices for higher-order reflection–refraction events.

## 2. Recurrence formulae for effective refractive indices

We assume the time-dependence of the incident electromagnetic wave in the form  $\exp(-i\omega t)$ , where  $\omega$  is the angular frequency,  $t$  is time, and  $i = (-1)^{1/2}$ . This definition of the time-dependent factor leads to a positive imaginary part of the index of refraction [13] such that  $m = m_r + im_i$  where  $m_r$  and  $m_i$  are the real and imaginary parts, respectively.

Fig. 1 schematically illustrates reflected and refracted ray paths associated with a certain incident ray. The terms  $P_j$  ( $j = 1, 2, 3, \dots$ ) indicate sequential incident points. If the refractive index for a particle is a real quantity (i.e., no absorption is involved), the directions of high-order reflected and refracted rays can be determined on the basis of the conventional Snell's law. However, if the refractive index of a particle is a complex quantity, Snell's law as a result of the phase continuity of the first-order incident and refractive waves in conjunction with wave transmission from air into the particle is given by

$$\sin \theta_t = \sin \theta_i / m, \tag{1}$$

where  $\theta_i$  and  $\theta_t$  are the incident and refractive angles, respectively. Clearly,  $\theta_t$  is a complex quantity if the imaginary part of  $m$  is nonzero. In this case,  $\theta_t$  does not have a simple geometric meaning in the context of geometric optics [13]. To carry out ray-tracing calculations in the case of an absorbing dielectric particle, Yang and Liou [14] defined an effective refractive index and expressed Snell's law in a real domain for the first-order reflection–refraction event. For self-completeness of the formulation in this study, we should briefly recapture the approach developed in [14], followed by deriving recurrence formulae for the effective refractive indices in the case of higher-order reflection–refraction events.

As shown in Fig. 2, the directions of the incident, reflected, and refracted rays for the first-order reflection–refraction event are denoted by unit vectors  $\hat{e}_{i,1}$ ,  $\hat{e}_{r,1}$ , and  $\hat{e}_{t,1}$ , respectively.  $\hat{n}_1$  is a unit vector normal locally to the particle surface at point  $P_1$  with its direction pointed into the particle. With the preceding definitions, the incident, reflected, and refracted electric field vectors can be expressed, respectively, via the following expressions [14]:

$$\vec{E}_{i,1}(\vec{r}, t) = \vec{E}_{i,1}(\vec{r}) \exp(-i\omega t), \tag{2}$$

$$\vec{E}_{r,1}(\vec{r}, t) = \vec{E}_{r,1}(\vec{r}) \exp(-i\omega t), \tag{3}$$

$$\vec{E}_{t,1}(\vec{r}, t) = \vec{E}_{t,1}(\vec{r}) \exp(-i\omega t), \tag{4}$$

where the spatial components of the electric field vectors are given by

$$\vec{E}_{i,1}(\vec{r}) = \vec{E}_{0i,1} \exp[ik_0 \hat{e}_{i,1} \cdot (\vec{r} - \vec{r}_{p,1})], \tag{5}$$

$$\vec{E}_{r,1}(\vec{r}) = \vec{E}_{0r,1} \exp[ik_0 \hat{e}_{r,1} \cdot (\vec{r} - \vec{r}_{p,1})], \tag{6}$$

$$\vec{E}_{t,1}(\vec{r}) = \vec{E}_{0t,1} \exp[ik_0 (N_{r,1} \hat{e}_{t,1} + iN_{n,1}^* \hat{n}_1) \cdot (\vec{r} - \vec{r}_{p,1})]. \tag{7}$$

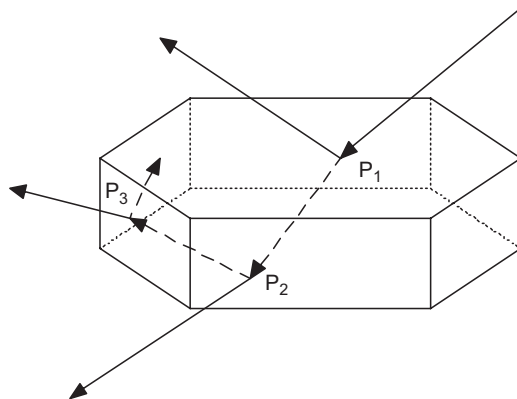


Fig. 1. A schematic illustration of the ray paths associated with an incident ray.

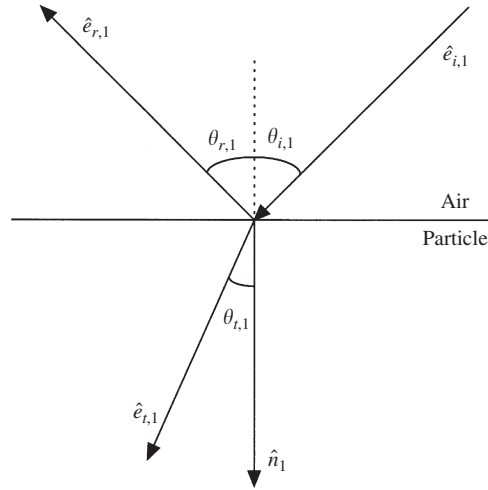


Fig. 2. Geometric configuration for the first-order reflection-refraction event when the ray transmission is from air into a scattering particle.

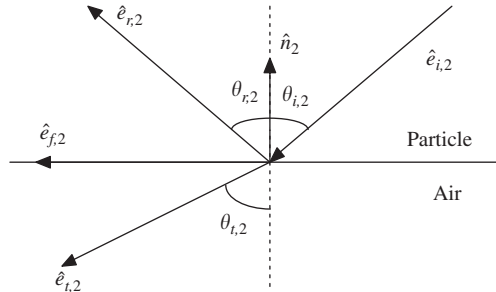


Fig. 3. Geometric configuration for the second-order reflection-refraction event when the ray transmission is from a scattering particle into air.

For a concise formulation, in the following discussions we will just consider the spatial components of the electric field vectors. In Eqs. (5)–(7),  $k_0 = 2\pi/\lambda_0$ ,  $\lambda_0$  is the incident wavelength,  $\vec{r}_{p,1}$  is the position vector of point  $P_1$ , and  $\vec{E}_{0i,1} = \vec{E}_0 \exp(ik_0 \hat{e}_{i,1} \cdot \vec{r}_{p,1})$  is the incident electric field vector at point  $P_1$ , where  $\vec{E}_0$  is the incident field electric amplitude vector. In Eq. (7), the terms  $N_{r,1}$  and  $N_{n,1}^*$  are the effective refractive indices given by [14,15]

$$N_{r,1} = 2^{-1/2} \{m_r^2 - m_i^2 + \sin^2 \theta_{i,1} + [(m_r^2 - m_i^2 - \sin^2 \theta_{i,1})^2 + 4m_r^2 m_i^2]^{1/2}\}^{1/2}, \quad (8)$$

$$N_{n,1}^* = 2^{-1/2} \{- (m_r^2 - m_i^2 - \sin^2 \theta_{i,1}) + [(m_r^2 - m_i^2 - \sin^2 \theta_{i,1})^2 + 4m_r^2 m_i^2]^{1/2}\}^{1/2}. \quad (9)$$

On the basis of this approach, Snell's law can be expressed as follows:

$$\theta_{r,1} = \theta_{i,1}, \quad (10)$$

$$\sin \theta_{t,1} = \sin \theta_{i,1} / N_{r,1}. \quad (11)$$

Fig. 3 shows the directions of the incident, reflected, and refracted rays for the second-order reflection-refraction event, which are denoted by unit vectors  $\hat{e}_{i,2}$ ,  $\hat{e}_{r,2}$ , and  $\hat{e}_{t,2}$ , respectively. Note that  $\hat{e}_{i,2} = \hat{e}_{t,1}$ ,  $\hat{n}_2$  is a unit vector normal to the particle surface at point  $P_2$  with its direction pointed into the particle, and  $\hat{e}_{f,2}$  is a unit vector parallel to both the incident plane and the particle surface at point  $P_2$ . The incident electric vector can then be written as follows:

$$\vec{E}_{i,2}(\vec{r}) = \vec{E}_{0i,2} \exp[ik_0(N_{r,1} \hat{e}_{i,2} + iN_{n,1}^* \hat{n}_1) \cdot (\vec{r} - \vec{r}_{p,2})], \quad (12)$$

where  $\vec{E}_{0i,2}$  is given by

$$\vec{E}_{0i,2}(\vec{r}) = \vec{E}_{0t,1} \exp[ik_0(N_{r,1} \hat{e}_{i,2} + iN_{n,1}^* \hat{n}_1) \cdot (\vec{r}_{p,2} - \vec{r}_{p,1})]. \quad (13)$$

In the ray-tracing calculation, tracing the propagation of the reflected or refracted ray is confined to the incident plane on which the position vector  $\vec{r} - \vec{r}_{p,2}$  is confined. With this constraint, this position vector can be decomposed

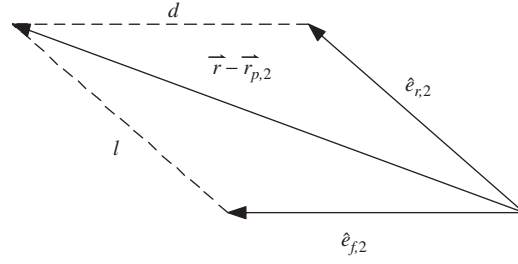


**Fig. 4.** Decomposition of a position vector  $\vec{r} - \vec{r}_{p,2}$  in terms of unit vectors  $\hat{e}_{f,2}$  and  $\hat{e}_{r,2}$ . The position vector is confined to the incident plane.

in the form

$$\vec{r} - \vec{r}_{p,2} = l\hat{e}_{r,2} + d\hat{e}_{f,2}, \quad (14)$$

where  $l$  and  $d$  are defined in Fig. 4. The reflected electric field vector at a location on the incident plane can be expressed as follows:

$$\vec{E}_{r,2}(\vec{r}) = \vec{E}_{0r,2} \exp\{ik_0[(N_{r,2}\hat{e}_{r,2} + iN_{n,2}^*\hat{n}_2) \cdot (l\hat{e}_{r,2} + d\hat{e}_{f,2}) + \delta_2]\}, \quad (15)$$

where  $\delta_2$  is a phase factor to be determined on the basis of the local phase continuity condition at the particle surface. Along the interface line (on the incident plane) between the particle and air, i.e.,  $l = 0$ , the phase of the incident wave must be the same as that of the reflected wave, which leads to the following phase continuity condition:

$$(N_{r,1}\hat{e}_{i,2} + iN_{n,1}^*\hat{n}_1) \cdot \hat{e}_{f,2}d = (N_{r,2}\hat{e}_{r,2} + iN_{n,2}^*\hat{n}_2) \cdot \hat{e}_{f,2}d + \delta_2. \quad (16)$$

It is evident from Fig. 3 that  $\hat{n}_2 \cdot \hat{e}_{f,2} = 0$ . Thus, if the particle face through point  $P_1$  is locally parallel to the particle face through point  $P_2$  (i.e.,  $\hat{n}_1 = -\hat{n}_2$ ), Eq. (16) reduces to

$$N_{r,1}\hat{e}_{i,2} \cdot \hat{e}_{f,2}d = N_{r,2}\hat{e}_{r,2} \cdot \hat{e}_{f,2}d + \delta_2. \quad (17)$$

Evidently,  $\delta_2$  in Eq. (17) reduces to zero if the following relation holds:

$$N_{r,1}\hat{e}_{i,2} \cdot \hat{e}_{f,2}d = N_{r,2}\hat{e}_{r,2} \cdot \hat{e}_{f,2}d. \quad (18)$$

Eq. (18) leads to a relationship between the incident and reflection angles, given by

$$N_{r,1} \sin \theta_{i,2} = N_{r,2} \sin \theta_{r,2}. \quad (19)$$

If  $\hat{n}_1$  is not parallel to  $\hat{n}_2$ , Eqs. (16) and (18) lead to the following relationship:

$$\delta_2 = iN_{n,1}^*\hat{n}_1 \cdot \hat{e}_{f,2}d. \quad (20)$$

Thus, the electric vector associated with the reflected ray, if observed on the incident plane, is given by

$$\vec{E}_{r,2}(\vec{r}) = \vec{E}_{0r,2} \exp\{ik_0[(N_{r,2}\hat{e}_{r,2} + iN_{n,2}^*\hat{n}_2) \cdot (l\hat{e}_{r,2} + d\hat{e}_{f,2}) + iN_{n,1}^*\hat{n}_1 \cdot \hat{e}_{f,2}d]\}. \quad (21)$$

The inhomogeneity properties of the electric vector given in Eq. (21) are quite complicated. For example, for a given  $k_0$ , the phase of the wave is determined by  $l$ ,  $d$ ,  $N_{r,2}$ ,  $\hat{e}_{f,2}$  and  $\hat{e}_{r,2}$ , whereas the decay of the amplitude of the wave is essentially determined by  $N_{n,1}^*$ ,  $\hat{n}_1$ ,  $N_{n,2}^*$ ,  $\hat{n}_2$ ,  $\hat{e}_{f,2}$ ,  $l$ , and  $d$ . Despite the intricacy of geometric vectors associated with phase and amplitude, tracing of the reflected ray is along the ray path in the direction specified by  $\hat{e}_{r,2}$ . For this reason, we have an expression in the vicinity of the reflected ray path under the condition given by Eq. (19), which is locally equivalent to Eq. (21) when  $d = 0$ , in the form:

$$\vec{E}(\vec{r}) = \vec{E}_{0r,2} \exp[ik_0(N_{r,2}\hat{e}_{r,2} + iN_{n,2}^*\hat{n}_2) \cdot (\vec{r} - \vec{r}_{p,2})]. \quad (22)$$

The electric vector in Eq. (22) must satisfy the wave equation within the particle medium given by

$$\nabla^2 \vec{E}(\vec{r}) + m^2 k_0^2 \vec{E}(\vec{r}) = 0. \quad (23)$$

Substituting Eq. (22) into Eq. (23), we have

$$N_{r,2}^2 - N_{n,2}^2 = m_r^2 - m_i^2, \quad (24)$$

$$N_{r,2}N_{n,2}^* \cos \theta_{r,2} = m_r m_i. \quad (25)$$

Combing Eq. (19) with Eqs. (24) and (25), we obtain the following solutions:

$$N_{r,2} = 2^{-1/2} \{m_r^2 - m_i^2 + N_{r,1}^2 \sin^2 \theta_{i,2} + [(m_r^2 - m_i^2 - N_{r,1}^2 \sin^2 \theta_{i,2})^2 + 4m_r^2 m_i^2]^{1/2}\}^{1/2}, \quad (26)$$

$$N_{n,2}^* = 2^{-1/2} \{ -(m_r^2 - m_i^2 - N_{r,1}^2 \sin^2 \theta_{i,2}) + [(m_r^2 - m_i^2 - N_{r,1}^2 \sin^2 \theta_{i,2})^2 + 4m_r^2 m_i^2]^{1/2} \}^{1/2}. \quad (27)$$

Furthermore, the refractive angle can be determined by the following expression:

$$\sin \theta_{t,2} = N_{r,1} \sin \theta_{i,2} = N_{r,2} \sin \theta_{r,2}. \quad (28)$$

Note that the total reflection occurs if  $N_{r,1} \sin \theta_{i,2} > 1$ .

Following the same procedure, the effective refractive indices for higher-order reflection–refraction events can be determined analytically and are given by

$$N_{r,j+1} = 2^{-1/2} \{ m_r^2 - m_i^2 + N_{r,j}^2 \sin^2 \theta_{i,j+1} + [(m_r^2 - m_i^2 - N_{r,j}^2 \sin^2 \theta_{i,j+1})^2 + 4m_r^2 m_i^2]^{1/2} \}^{1/2}, \quad (29)$$

$$N_{n,j+1}^* = 2^{-1/2} \{ -(m_r^2 - m_i^2 - N_{r,j}^2 \sin^2 \theta_{i,j+1}) + [(m_r^2 - m_i^2 - N_{r,j}^2 \sin^2 \theta_{i,j+1})^2 + 4m_r^2 m_i^2]^{1/2} \}^{1/2}, \quad (30)$$

where the subscript  $j$  ( $j \geq 2$ ) represents the order of reflection–refraction events. Subsequently, Snell's law, expressed in terms of the effective refractive indices, can be rewritten as follows:

$$N_{r,j} \sin \theta_{i,j+1} = N_{r,j+1} \sin \theta_{r,j+1}, \quad (31)$$

$$N_{r,j} \sin \theta_{i,j+1} = \sin \theta_{t,j+1}. \quad (32)$$

Along the ray path within an absorbing particle, the electric field vectors can then be expressed by

$$\vec{E}_{t,1}(\vec{r})|_{\vec{r}=\hat{e}_{t,1}+\vec{r}_{p,1}} = \vec{E}_{0t,1} \exp(-N_{n,1}^* \cos \theta_{t,1} l) \exp(ik_0 N_{r,1} l), \quad (33)$$

$$\vec{E}_{r,j}(\vec{r})|_{\vec{r}=\hat{e}_{r,j}+\vec{r}_{p,j}} = \vec{E}_{0r,j} \exp(-N_{n,j}^* \cos \theta_{r,j} l) \exp(ik_0 N_{r,j} l), \quad j = 2, 3, 4, \dots \quad (34)$$

It is evident from Eqs. (33) and (34) that  $N_{r,j}$  ( $j = 1, 2, 3, \dots$ ) determines the phase of the wave, while  $N_{n,1}^* \cos \theta_{t,1}$  and  $N_{n,j}^* \cos \theta_{r,j}$  denote the absorption along ray propagation. Thus, the former is the real part of the effective index of refraction, while the latter two parameters represent its imaginary part. We denote the imaginary part ( $N_{n,j}$ ,  $j = 1, 2, 3, \dots$ ) of the effective refractive index as follows:

$$N_{n,1} = N_{n,1}^* \cos \theta_{t,1}, \quad (35)$$

$$N_{n,j} = N_{n,j}^* \cos \theta_{r,j}, \quad j = 2, 3, 4, \dots \quad (36)$$

### 3. Numerical results

In the numerical calculation involved in the ray-tracing procedure, it is convenient to trace the directions of reflected and refracted rays via vector equations that are independent of a specific coordinate system. From Eqs. (10), (11), (31) and (32) as well as the geometrical configurations shown in Figs. 2 and 3, we obtain

$$\hat{e}_{r,1} = \hat{e}_{i,1} - (\cos \theta_{i,1} + \cos \theta_{r,1}) \hat{n}_1, \quad (37)$$

$$\hat{e}_{t,1} = \hat{e}_{i,1} / N_{r,1} - (\cos \theta_{i,1} / N_{r,1} - \cos \theta_{t,1}) \hat{n}_1, \quad (38)$$

$$\hat{e}_{r,j} = \frac{N_{r,j-1}}{N_{r,j}} \hat{e}_{i,j} - \left( \cos \theta_{r,j} + \frac{N_{r,j-1}}{N_{r,j}} \cos \theta_{i,j} \right) \hat{n}_j, \quad j = 2, 3, 4, \dots \quad (39)$$

$$\hat{e}_{t,j} = N_{r,j-1} \hat{e}_{i,j} - (N_{r,j-1} \cos \theta_{i,j} - \cos \theta_{t,j}) \hat{n}_j, \quad j = 2, 3, 4, \dots \text{ (if total reflection does not occur)}. \quad (40)$$

To illustrate the effect of using the effective refractive index on the determination of a ray path, panel (a) in Fig. 5 shows a two-dimensional (2D) case concerning the propagation of an incident ray that impinges on a hexagon. The complex index of refraction of the 2D particle is assumed to be  $1.3857+i0.422$ , the refractive index of ice at a wavelength of  $12.5 \mu\text{m}$  [16]. Panel (b) is similar to panel (a) except that the complex index of refraction of the 2D particle is assumed to be  $1.0925+i0.248$ , the refractive index of ice at a wavelength of  $11.0 \mu\text{m}$  [16]. For the computation, the incident angle for the first-order reflection–refraction event is assumed to be  $65^\circ$  and  $55^\circ$  (i.e.,  $\theta_{i,1} + \theta_{r,1} = 130^\circ$  and  $110^\circ$ , as shown in Fig. 5) for panels (a) and (b), respectively. In Fig. 5, the solid lines denote the results computed by using the effective refractive indices for corresponding orders of reflection–refraction events. The dotted lines indicate the results computed from simplified Snell's law given by

$$\theta_{i,j} = \theta_{r,j}, \quad j = 1, 2, 3, \dots$$

$$\sin \theta_{t,1} = \sin \theta_{i,1} / m_r, \quad (41)$$

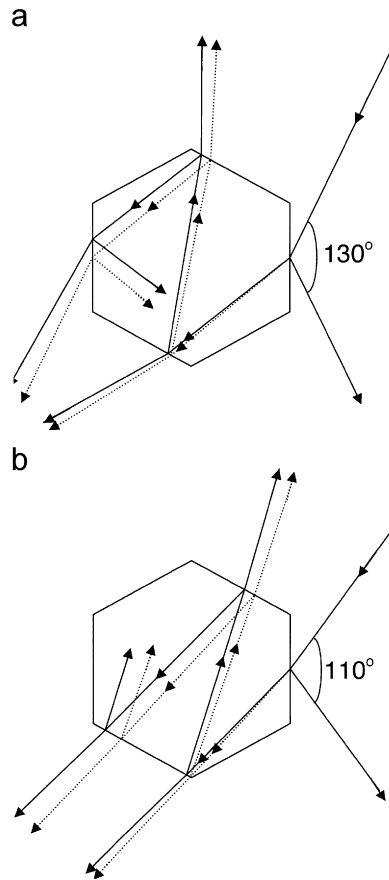


**Fig. 5.** The solid lines are calculated on the basis of the effective refractive indices and the dotted lines are based on simplified Snell's law given by  $\sin \theta_{t,1} = \sin \theta_{i,1}/m_r$  and  $\sin \theta_{t,j} = m_r \sin \theta_{i,j}$ ,  $j = 2,3,4 \dots$ . In the calculation, the inherent complex index of refraction of the particle is assumed to be  $1.3857+i0.422$  and  $1.0925+i0.248$  for panels (a) and (b), respectively.

**Table 1**

The real and imaginary parts of the effective index of refraction for various orders of the reflection–refraction events illustrated in Fig. 5. Cases 1 and 2 in the table correspond to panels a and b in Fig. 5, respectively.

Order of reflection–refraction events	Case 1 $m_r = 1.3857$ and $m_i = 0.422$ $\theta_{i,1} = 65^\circ$		Case 2 $m_r = 1.0925$ and $m_i = 0.248$ $\theta_{i,1} = 55^\circ$	
	$N_{r,j}$	$N_{n,j}$	$N_{r,j}$	$N_{r,j}$
1	1.4234	0.41083	1.1213	0.24163
2	1.3942	0.41944	1.0940	0.24766
3	1.3942	0.41944	1.0940	0.24766
4	1.4202	0.41175	1.0940	0.24766
5	1.3953	0.41910	1.1183	0.24227

$$\sin \theta_{t,j} = m_r \sin \theta_{i,j}, \quad j = 2, 3, 4 \dots \text{ (if total reflection does not occur).} \tag{42}$$

It is evident from Fig. 5 that the effect of wave inhomogeneity on the propagation of a localized wave (or a ray) is quite substantial for higher-order reflection–refraction events. However, the effect of the wave inhomogeneity on the scattering properties of the particle may be small. This is because the wave inhomogeneity is significant only when the absorption of the particle is substantial. For a strongly absorbing particle, the energy carried by a higher-order ray is much less than the carried by a lower-order ray. In this case, diffraction and external reflection processes dominate the scattered field.

Table 1 lists the real and imaginary parts of the effective index of refraction for two cases. Cases 1 and 2 in the table correspond to panels (a) and (b) in Fig. 5, respectively. We note from Table 1 that the  $N_{r,j}$  and  $N_{n,j}$  are larger and smaller than  $m_r$  and  $m_i$ , respectively. The dependence of the effective index of refraction on ray history is also evident from the results

listed in Table 1. There is no systematic change in  $N_{rj}$  and  $N_{nj}$  as a function of the order of reflection–refraction events. By matching the order of reflection–refraction events for the results in Table 1 with the geometries defined in Fig. 5, it is noticed that the effective refractive indices for two sequential internal reflections are the same if the two particle faces for these reflections are parallel. Evidently, the effective refractive indices depend on both ray history and particle shape.

#### 4. Summary

The electromagnetic waves refracted into an absorbing medium are inhomogeneous under which the conventional Snell's law will involve a complex refractive angle that does not have a general geometric meaning in the context of geometric optics. As a follow-up to our previous work [14], we derived recurrence formulae for the effective refractive index to account for ray propagation within an absorption particle. Although the inhomogeneous electromagnetic wave associated with an internally reflected ray is quite complicated, the mathematical expression of this wave in the vicinity of the corresponding ray path confined to the incident plane can be simplified. Using the concept of effective refractive index, Snell's law can be expressed in a real form and is suitable for ray-tracing calculations. The present numerical results show that the effective index of refraction can be quite different from the inherent index of refraction of a strongly absorbing particle. If the particle faces for two sequential internal reflections are parallel to each other, the corresponding effective refractive indices are the same. The effective refractive index associated with an internal ray depends on both the history of this ray and the geometry of the corresponding scattering particle. To fully understand the wave inhomogeneity effect on the single-scattering properties of an absorbing particle, we need to consider the effects of wave inhomogeneity on both ray propagation and Fresnel coefficients in the ray-tracing calculation, an involved subject requiring future studies.

#### Acknowledgments

This study was supported by the National Science Foundation under grants ATM-0239605 and ATM-0331550. We thank H.-M. Cho for assistance in figure preparation.

#### References

- [1] Mishchenko MI, Wiscombe WJ, Hovenier JW, Travis LD. Overview of scattering by nonspherical particles. In: Mishchenko MI, Hovenier JW, Travis LD, editors. Light scattering by nonspherical particles: theory, measurements, and geophysical applications. San Diego, CA: Academic Press; 2000. p. 29–60.
- [2] Takano Y, Liou KN. Solar radiative transfer in cirrus clouds. Part I. Single-scattering and optical properties of hexagonal ice crystals. *J Atmos Sci* 1989;46:3–19.
- [3] Muinonen K. Scattering of light by crystals: a modified Kirchhoff approximation. *Appl Opt* 1989;28:3044–50.
- [4] Macke A. Scattering of light by polyhedral ice crystals. *Appl Opt* 1993;32:2780–8.
- [5] Iaquinia J, Isaka H, Personne P. Scattering phase function of bullet rosette ice crystals. *J Atmos Sci* 1995;52:1401–13.
- [6] Macke A, Mueller J, Raschke E. Single scattering properties of atmospheric ice crystal. *J Atmos Sci* 1996;53:2813–25.
- [7] Yang P, Liou KN. Geometric-optics-integral-equation method for light scattering by nonspherical ice crystals. *Appl Opt* 1996;35:6568–84.
- [8] Labonnote CL, Brogniez G, Doutriaux-Boucher M, Buriez JC, Gayet JF, Chepfer H. Modeling of light in cirrus clouds with inhomogeneous hexagonal monocrystals: comparison with in-situ and ADEOS-POLDER measurements. *Geophys Res Lett* 2000;27:113–6.
- [9] Borovoi AG, Grishin IA. Scattering matrices for large ice crystal particles. *J Opt Soc Am A* 2003;20:2071–80.
- [10] Um J, McFarquhar GM. Single-scattering properties of aggregates of bullet rosettes in cirrus. *J Appl Meteor Climatol* 2007;46:757–75.
- [11] Nousiainen T, Muinonen K, Raisanen P. Scattering of light by large Saharan dust particles in a modified ray optics approximation. *J Geophys Res* 2003;108(D1):4025.
- [12] Yang P, Feng Q, Hong G, Kattawar GW, Wiscombe WJ, Mishchenko MI, et al. Modeling of the scattering and radiative properties of nonspherical dust particles. *J Aerosol Sci* 2007;38:995–1014.
- [13] Bohren CF, Huffman DR. Absorption and scattering of light by small particles. New York: Wiley; 1983.
- [14] Yang P, Liou KN. Light scattering by hexagonal ice crystals: comparison of finite-difference time domain and geometric optics methods. *J Opt Soc Am A* 1995;12:162–76.
- [15] Yang P, Gao BC, Baum BA, Wiscombe W, Mishchenko MI, Winker DM, et al. Asymptotic solutions of optical properties of large particles with strong absorption. *Appl Opt* 2001;40:1532–47.
- [16] Warren SG. Optical constants of ice from the ultraviolet to the microwave. *Appl Opt* 1984;23:1206–25.